Higuchi *et al. Journal of Wood Science* (2023) 69:27
https://doi.org/10.1186/s10086-023-02102-4

Journal of Wood Science

ORIGINAL ARTICLE

Open Access

The "chi-chi" of *Ginkgo biloba* L. grows downward with horizontally curving tracheids having compression-wood-like features

Seiichi Higuchi[1], Dan Aoki[1*], Yasuyuki Matsushita[1,2], Masato Yoshida[1], Sachie Yagami[1] and Kazuhiko Fukushima[1]

Abstract

The old *Ginkgo biloba* L. trees often develop cylindrical woody structures that grow downward from the underside of the large branches near the trunks. This structure is traditionally called "chi-chi" (a breast) in Japan. The structure of chi-chi has not been investigated in detail because of the rarity of such old trees of *G. biloba*. This study examined the chi-chi from wood anatomy and chemistry viewpoints. After debarking, there were many woody bulges and latent buds. There were hollows corresponding to these latent buds on the inner side of the bark. In the transverse section obtained from the tip part of the chi-chi sample, we found tracheids curving in a horizontal plane, and the parenchymatous latent bud tissue is the center of the swirl. Microscopic observations and X-ray micro-computed tomography suggest the growing course of the chi-chi due to several swirls contiguous to each other. From these observations, the downward growth of the chi-chi starting from the cambium cell division might be driven by the woody bulges with latent buds. The cell walls of the curved tracheids were not thickened, not rounded, and had no intercellular spaces, but their S_3 layers disappeared. Furthermore, the results of thioacidolysis and acetyl bromide analyses exhibited *p*-hydroxyphenyl subunits deposition to lignin and high lignin content on the tip part of the chi-chi. These results suggest that the curved tracheids in the chi-chi have compression-wood-like properties to some extent.

Keywords Ginkgo, Chi-chi, Abnormal tracheid shapes, Swirling, Gravity direction, Phloroglucinol, Bordered pits, Ray cells

Introduction

The old *Ginkgo biloba* L. trees often develop cylindrical woody structures that grow downwards from the underside of the large branches near the trunks (Fig. 1). Traditionally, this tissue is called "chi-chi" (a breast) and has been a folk belief on childbirth and lactation in Japan. After an extended period, they grow downward to over 1 m long. When grown down to the ground, they take roots and produce vegetative shoots [1] (Additional file 1: Fig. S1). The same cylindrical woody structures of ginkgo are called "zhongru" (stalactite) in China. Li and Lin examined the chi-chi anatomically, found that some of the tracheids were arranged in whirls in the tangential section, and described it as the abnormal growth of coniferous trees [2]. Barlow and Kurczyńska used the word "chi-chi" as a name of the tissue and concluded that a chi-chi uses the vascular cambium not only for its widening growth but also for its elongation [3]. Del Tredici studied the chi-chi found at the underground level ("a basal chi-chi") and concluded that vegetative regeneration using

*Correspondence:
Dan Aoki
aoki.dan@nagoya-u.jp
[1] Graduate School of Bioagricultural Sciences, Nagoya University, Nagoya 464-8601, Japan
[2] Present Address: Institute of Agriculture, Tokyo University of Agriculture and Technology, Tokyo 183-8509, Japan

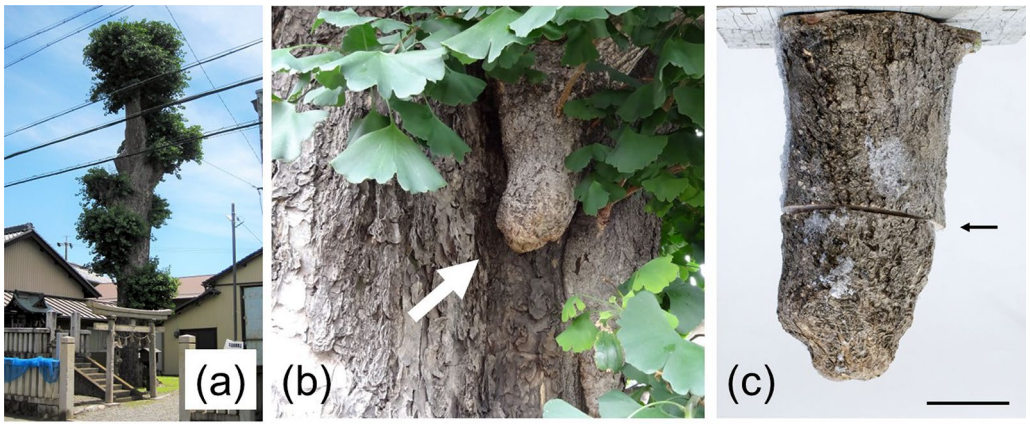

Fig. 1 The chi-chi sample overview. **a** The *G. biloba* tree in Akiba shrine in 2023. **b** Chi-chi of *G. biloba* growing downward near the trunk (white arrow). **c** Sampled chi-chi. The tip part was cut off at the black arrow and used for research. Scale bar, 5 cm

the basal chi-chi may have played a role in the remarkable survival of the genus *Ginkgo* since the Cretaceous. He also discussed that a basal chi-chi is identical to an aerial chi-chi [4]. The aerial chi-chi is the same one called "chi-chi" in our study.

Regarding anatomical characteristics of gymnosperms, they usually produce specific tissues, so-called compression wood, to push stems upwards on the underside of the leaning stems. The branches of the gymnosperm also have compression wood on their underside. *G. biloba* is similar to modern conifer and develops compression wood [5–7]. Compression wood tracheids are thick-walled and rounded in cross-section, resulting in intercellular spaces between the corners of adjoining cells. While the cellulose microfibril angle (MFA) of normal wood tracheids is low (~ 10°), the thickened S_2 cell wall layer has an increased MFA (30–50°) [7, 8]. The S_3 wall layer is frequently absent in compression wood.

As for the compositional differences in compression wood, secondary cell walls reduce polysaccharides and increase lignin. Lignin is an indispensable substance for vascular plants. The principal function of lignin in plants is to assist in water movement; lignin forms a barrier for evaporation and, thus, helps channel water to critical areas of the plant. Lignin is an aromatic heteropolymer built up by the combination of three basic monomer types of *p*-coumaryl alcohol (H), coniferyl alcohol (G), and sinapyl alcohol (S). Generally, H-unit is a minor structural unit found in the compression wood and grasses, G-unit is the main structural unit in softwood (gymnosperm) lignin and the second most unit in hardwood (angiosperms) lignin, and S-unit is the most abundant structural unit in angiosperm lignin [9]. *G. biloba* is a gymnosperm, so it mainly has a G-unit and contains H-unit only in the compression wood. However, as Uzal et al. found the presence of S-unit in *G. biloba* cell cultures [10], the biosynthetic mechanisms of plant lignin are flexible and complex.

As described above, the cell wall structures and lignin chemical structures provide essential information about the tissue. However, the detailed cell wall structures of the chi-chi have yet to be reported as far as we know, although abnormal tracheid shapes were reported [2]. Also, there is no study on the lignin of the chi-chi. Therefore, this study examined the chi-chi using microscopic observations using scanning electron microscopy (SEM), field-emission SEM (FE-SEM), optical microscopy with staining, and X-ray micro-computed tomography (X-ray μCT). Further, the content and the chemical structures of lignin were evaluated using the acetyl bromide and thioacidolysis methods, respectively. Our purpose is to reveal how the chi-chi grow downward and how are the cell wall structure and lignin chemical structures in the tissue.

Materials and methods

Sample preparation

Generally, most elder ginkgo trees growing on the premises of Shinto shrines and Buddhist temples are designated as national monuments by the government or natural monuments by local governments. Therefore, it is difficult to obtain a chi-chi as an experimental material in Japan. Fortunately, we got an opportunity to sample the chi-chi, which was not a designated natural monument (Fig. 1).

On June 21st, 2012, over 20 cm long chi-chi was cut from the trunk of a *G. biloba* tree growing in the premises of Akiba shrine (35°22′18″ N, 136°45′42″ E) in Kasamatsu town, Gifu prefecture, Japan (Fig. 1a). The height and the diameter at breast height of the ginkgo tree were evaluated as about 25 m and 119 cm, respectively, by the

Educational Committee of Kasamatsu town in 2016. The tree age was not correctly evaluated, but the committee estimated it as over 200 years old. In addition, lateral shoots near the chi-chi were also sampled. The samples were carried to Nagoya University and frozen with liquid nitrogen. Next, the chi-chi of the tip part was cut to 9.5 cm long (Fig. 1b) and cut in half longitudinally. Then, several samples were cut from the chi-chi and named samples A, B, C, D, and E (Fig. 2). The sample E surface was polished with a polishing paper (Sankyo Chemical, Super Precision Polishing Film #1000). The polished surface of the longitudinal half block (sample E) is shown in Fig. 2.

Sample A was observed by SEM and then was cut into four pieces, A-1, A-2, A-3, and A-4 (Fig. 3a and b). The samples A-1 and A-3 were sliced to tangential sections of 0.1 mm thickness with sliding microtome (REM-710, Yamato kohki, Asaka, Japan) and used for lignin analysis after extraction by ethanol/benzene (1:2, *v*/*v*) over 10 h in a Soxhlet extractor. Sample A-2 was used for FE-SEM observation. The upper part of the chi-chi (sample B) was used for SEM observation after debarking. After SEM observation, sample B was similarly used for lignin analysis after the same procedures used for sample A-1. The lowest tip part of the chi-chi (sample C) was cut to a 1 cm × 1 cm diamond-shaped × 3 cm

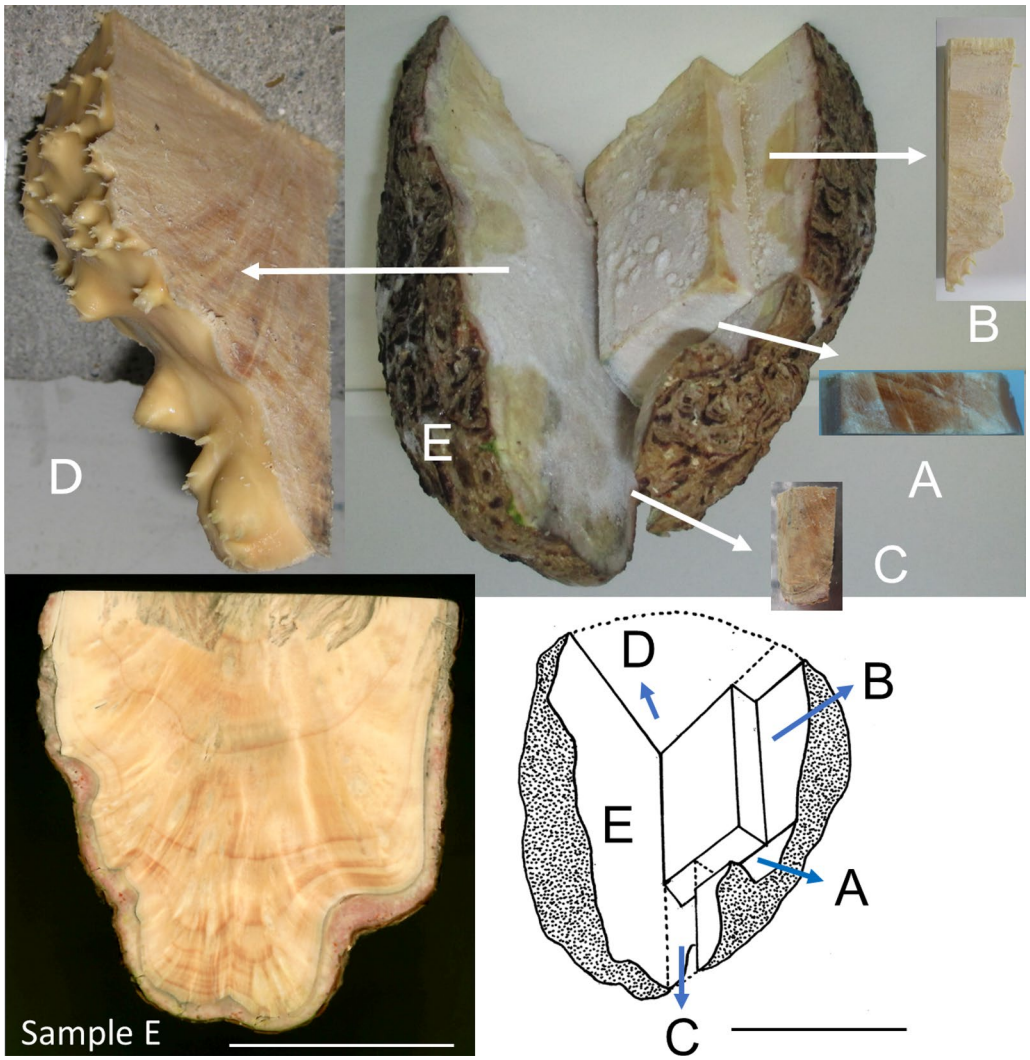

Fig. 2 Diagram showing how the samples were cut off from the chi-chi. **A** Used for SEM, FE-SEM, and thioacidolysis. **B** Used for SEM and thioacidolysis. **C** Used for X-ray CT, optical microscopy, and SEM. **D** Used for thioacidolysis and lignin determination. **E** Used for scanning the surface of the longitudinal half section. The lower left image is the polished surface of the sample E. Scale bars, 5 cm

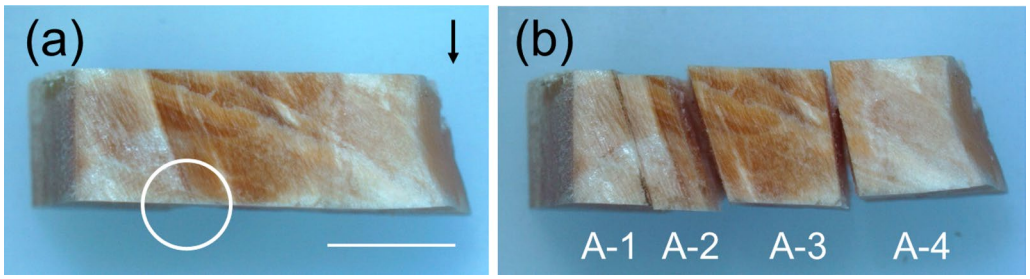

Fig. 3 The sample A cutting diagram for SEM and FE-SEM observations. **a** Radial view of sample A. A white circle indicates the area observed by SEM from the front and the underside. A black arrow indicates the direction of gravity. Scale bar, 5 mm. **b** Sample A was cut into 4 pieces, A-1, A-2, A-3, and A-4. Samples A-1 and A-3 were used for lignin analysis. Sample A-2 was used for FE-SEM observation

height block and used for X-ray μCT, optical microscopy, and SEM observations.

One-sixth of the tip part of the chi-chi (sample D) was debarked and cut into 17 pieces of 5 mm thickness with a jigsaw (Fig. 4a). Then, No.1, No.5, No.9, No.13, and No.17 boards suggested in Fig. 4a were cut to small blocks of Da, Db, Dc, Dd, De, Df, Dg, Dh, Di, Dj, Dk, and Dl as schematically illustrated in Fig. 4b. Each block was similarly used for lignin analysis after the same procedures used for the sample A-1. Next, lateral shoots were cut to 30 mm in length and debarked. Then, the shoots were cut to separate the lower and upper parts. Each sample was similarly used for lignin analysis after the same procedures used for sample A-1.

Scanning electron microscopy (SEM) and field-emission (FE) SEM

The samples were hydrated in the water at room temperature and planed off their surfaces with a sliding microtome. After drying in a vacuum oven at 40 ℃, samples were observed using SEM (S-3400N-T3, Hitachi, Japan) without any surface metal coating. FE-SEM (S-4500, Hitachi, Japan) was used to confirm the existence of the S_3 layer in the middle part of the chi-chi (sample A-2). The sample was prepared in the same manner

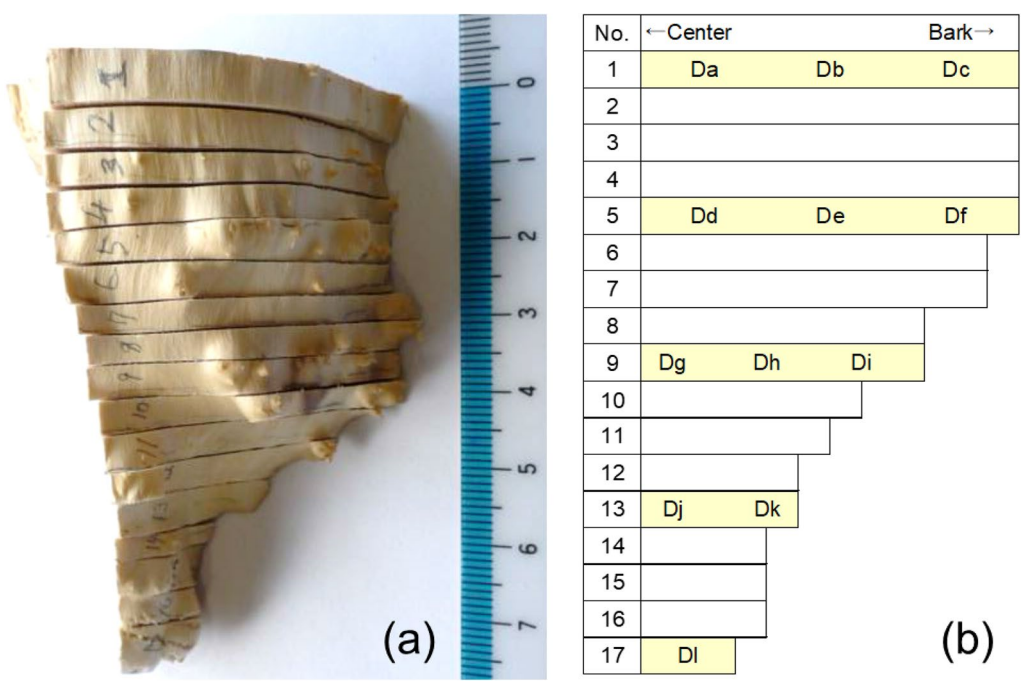

Fig. 4 The sample D cutting diagram for thioacidolysis analyses. **a** Cut boards from 1 to 17. The board No. 1 is the uppermost part, and the board No. 17 is the lowest part. The ruler unit is cm. **b** The schematically illustrated locations for the thioacidolysis samples of Da, Db, Dc, Dd, De, Df, Dg, Dh, Di, Dj, Dk, and Dl

as that described above. Before the observations, the surface was coated with Pd–Pt (E-1030 Ion Sputter, Hitachi, Japan). Then, the coated sample was observed with FE-SEM.

X-ray micro-computed tomography (X-ray μCT)

The computed tomographic images of the lowest tip part of the chi-chi (sample C) were obtained by X-ray μCT analysis (Sky Scan 1272, Bruker, Belgium). The measurement conditions are as follows: beam source, 50 kV 200 μA; exposure, 481 ms; rotation step, 0.1 deg; image pixel size, 3.0 μm; measurement time 15 h 45 min; reconstruction time of 8802 slices, 35 h 37 min; result image size, 4904 × 4904 pixels. Slice images were obtained from the reconstructed data as 964 × 917 pixels in gif format. The gif animation file was converted to a movie file and embedded in the Additional file 2.

Lignin content evaluation by the acetyl bromide method

The extractive-free sections sliced 0.1 mm thickness was used for lignin determination by the acetyl bromide method [11, 12]. The lignin content of the samples was determined by measuring the absorbances at 280 nm using a lignin absorption coefficient of 21.0 L g^{-1} cm^{-1} which was obtained by using the milled wood lignin (MWL) of ginkgo. The MWL was prepared from the stem of a ginkgo 19-year-old tree grown in the Nagoya University experimental farm (Nagoya, Japan). The absorbance was measured by a UV spectrometer (V-530, JASCO, Japan).

Thioacidolysis and gas chromatography–mass spectrometry (GC–MS)

Thioacidolysis selectively cleaves the β-aryl ether bonds of lignin. Therefore, the analysis of the lignin-derived monomeric products can evaluate the type and amount of the lignin structural units only involved in β-aryl ether bonds [13]. Furthermore, the lignin-derived dimers are obtained after desulfurization of the thioacidolysis products over Laney nickel [14, 15].

The extractive-free sections sliced 0.1 mm thickness was used for thioacidolysis. Thioacidolysis and desulfurization were carried out according to the method reported by Lapierre et al. [14, 15]. Approximately, 5 mg of the different sliced dry sections were placed in a 5 mL dioxane/ethanethiol mixture (8.75:1, *v*/*v*) and 0.2 M BF_3 etherate in a tube fitted with a Teflon-lined screwcap. An internal standard (docosane, 0.05 mg) was added to the sample tube. Then, the sample was heated at 100 °C for 4 h, shaking mildly for a minute at intervals of 30 min. The reaction mixture was cooled on ice, and 4 mL $NaHCO_3$ aqueous solution (0.4 M) was added to stop the reaction. The pH of the mixture was adjusted to 2–3 with HCl aqueous solution (1:3, *v*/*v*), and the entire mixture was extracted using CH_2Cl_2 (5 mL × 3 times). The combined organic extracts were dried over Na_2SO_4 and evaporated under reduced pressure at 40 °C. The final residue was diluted in 1.0 mL CH_2Cl_2 and stored at 4 °C in a vial. Three replications were performed for every sample.

For desulfurization, 0.5 mL of the thioacidolysis CH_2Cl_2 solution was treated with 1.5 mL Raney nickel aqueous slurry and 2.5 mL dioxane in a glass tube fitted with a Tefron-lined screwcap. Desulfurization was carried out at 50 °C for 4 h with shaking at intervals of 30 min. The tube was cooled on ice, and the supernatant solution of the reaction mixture was moved into another tube. Then the pH of the solution was adjusted to 3–4 with HCl aqueous solution (1:3, *v*/*v*), and the entire mixture was extracted using CH_2Cl_2 (5 mL × 3 times). The combined organic extracts were dried over Na_2SO_4 and evaporated under reduced pressure at 40 °C. The final residue was diluted in 1.0 mL CH_2Cl_2 and stored at 4 °C in a vial. Three replications were performed for every sample.

The final CH_2Cl_2 solution of lignin monomeric or dimeric products was silylated with *N*,*O*-bis(trimethylsilyl) trifluoroacetoamide and pyridine. The silylated derivatives were analyzed by GC–MS (QP2010, Shimadzu, Japan). Measurement conditions for monomeric products: capillary column, Rtx-1 of inner diameter, 0.32 mm × 30 m, film thickness 0.25 μm; injection temperature, 250 °C; temperature program, from 180 to 230 °C at 2 °C/min, to 250 °C at 15 °C/min, and hold 10 min; carrier gas, He (1.36 mL/min). For dimeric products: temperature program, from 180 to 240 °C at 2 °C/min, to 280 °C at 1 °C/min, and hold 10 min. A response factor 1.5 was used for monomeric products, and 1.0 was used for dimeric products. Three measurements were conducted for every sample.

Results

Morphological features

The chi-chi sample extended downward from a branch near the trunk and was 25 cm long. It was cylindrical and covered with bark to the tip as described by Fujii [1] (Figs. 1b, c, 2). After debarking, there were many woody bulges and latent buds (Fig. 2D). In Fig. 2D, the bulges have plural buds; therefore, the buds seemed to be in the upper part but not always at the tip of the bulges. The latent buds are parenchymatous tissue and diminished after debarking and drying (Additional file 1: Fig. S2, S3). On the inner surface of the bark, there were hollows corresponding to the position where the latent buds were present (Additional file 1: Fig. S2d). Sample A, used for SEM, FE-SEM, and lignin analysis, also had downward extending woody bulges before the lower part was cut (Additional file 1: Fig. S4).

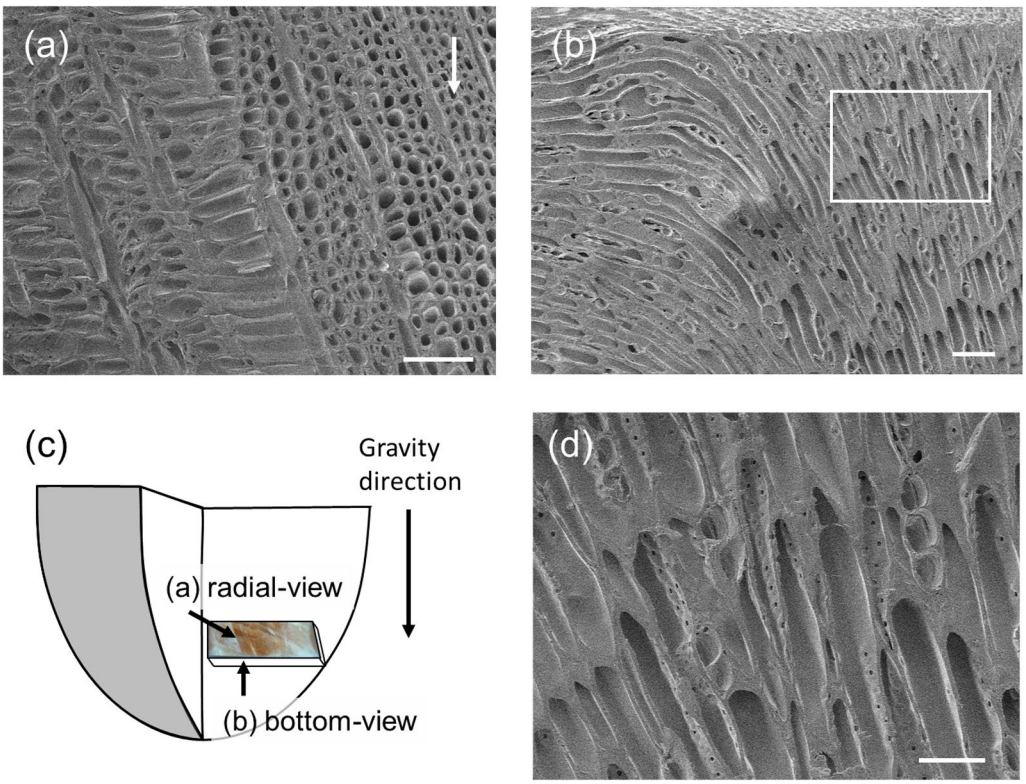

Fig. 5 SEM micrograph of the radial and bottom views of sample A. **a** An image was taken from the radial view at the white circle in Fig. 3a. The right side of the image shows the transverse surface of the tracheids, and the left side of the image displays the longitudinal surface of the tracheids. A white arrow indicates the direction of gravity. Scale bar, 100 µm. **b** An image taken from the bottom-view at the white circle in Fig. 3a. The left side of the image shows the tracheids curving in a horizontal plane. The direction of gravity is from the reverse side to the front side. Scale bar, 100 µm. **c** The schematic illustration of the observation angles to sample A for (**a**) and (**b**) images. **d** An enlarged image of the zone outlined by the white rectangular area in (**b**) suggests that tracheids have bordered pits. Scale bar, 50 µm

Horizontally curving tracheids

A clear boundary between the light brown and dark brown areas was observed in the left 1/3 part of sample A (Fig. 3a). Figure 5a shows a radial-view SEM image of the boundary, and a white arrow indicates the direction of gravity. The same sample block of A-2 was observed from a different angle and shown in Fig. 5b. The observation angles and relationships are schematically illustrated in Fig. 5c. The SEM image in Fig. 5d is an enlarged image of the area framed by the white rectangle in Fig. 5b and shows that the tracheids have bordered pits.

These images show that the tracheids in the growing part of chi-chi (block A) are horizontally (perpendicular to the gravity direction) curving. Furthermore, as shown in Additional file 1: Fig. S3, the center of the tracheid swirling might be the parenchymatous latent bud tissue.

In the case of sample B, taken from the upper and bark-side part of the chi-chi sample (Fig. 2), the tracheids aligned parallel to the gravity direction (Fig. 6). Therefore, ca. 10 cm far from the tip of the chi-chi, gravity-parallel

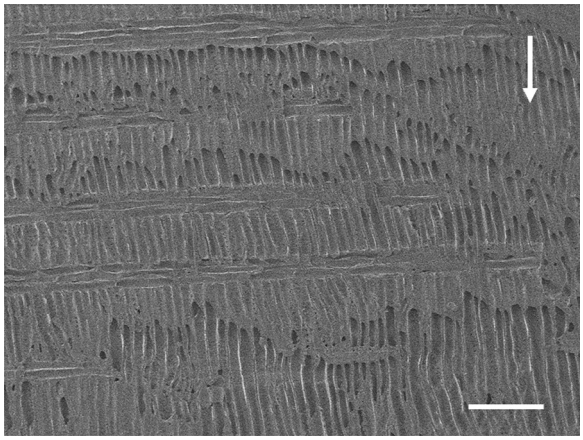

Fig. 6 SEM micrograph of the upper part of sample B near the bark. Tracheids are lining up parallel with gravity. The white arrow indicates the direction of gravity. Scale bar, 200 µm

tracheids are generated by the cambium, similar to those in normal trunks.

Cell wall structures of the curving tracheids

An FE-SEM image of sample A-2 taken from the lumen side is shown in Fig. 7. The image shows no S_3 layer in the cell wall layer structure and that the S_2 layer microfibril orientation is 45°. However, as shown in Fig. 5, other features commonly observed in a gymnosperm compression wood, such as cell wall thickening, the rounded tracheid shape, and the development of intercellular spaces, were not observed. The comparable images of the cell walls of vertical (in sample B) or horizontal (in sample A-2) tracheids are summarized in Additional file 1: Fig. S5.

Wood formation with swirls

Sample C was taken from the central tip of the chi-chi (Fig. 2). SEM images of the horizontal plane at 30 mm apart from the tip (sample C) are shown in Fig. 8. In Fig. 8a, tracheids curved and spirally aligned as a swirl. In the same sample block C, a wide-angle view displays that several swirls are contiguous to each other (Fig. 8b). The center of the swirl in Fig. 8a has an aggregate of parenchyma cells (Enlarged and displayed in Additional file 1: Fig. S6). However, it was unclear how the curving started or whether it had a pith-like tissue.

The enlarged SEM image of the area suggested by white rectangles in Fig. 8c shows that curving tracheids have bordered pits (Fig. 8d). In Fig. 8d, cytoplasmic debris are seen in uniseriate ray. Here, these ray cells intersected the horizontally curving tracheids; therefore, the axis of the ray cells was parallel to the gravity direction.

To understand the internal 3D wood formation in the chi-chi, sample C was observed by X-ray μCT. An animation created by moving the horizontally sliced plane is shown in Additional file 2: Fig. S7. Several swirls, in which tracheids were assembled in a spiral shape, were observed to be continuous over millimeters long in the vertical direction and forming wood as multiple swirls contiguous to each other. As for the swirl center, Additional file 1: Fig. S3 shows that the parenchymatous latent bud tissue is the center of the tracheid swirling.

Lignin chemical structures

The leading tip part of the chi-chi sample C was cut to a 20 μm thick section in the longitudinal direction. The phloroglucinol HCl-stained optical microscope image is shown in Fig. 9. On the left side of the image, the tracheids with bordered pits are formed horizontally. The tracheids in different directions can be seen on the right side of the image. The lower part of the image is the bark side, and the reddish-purple color becomes darker toward the upper part, reflecting the progress of lignification.

First, a quantitative comparison was made by the acetyl bromide method (Additional file 1: Table S1). The Dh, Dj, Dk, and Dl samples resulted in the lignin content of 30.8–33.7%, with an average value of 32.6%, which tended to be higher than the average value of 31.5% obtained for the other part of samples, where no H lignin units were detected as described below. The amount of lignin in the lower part of the Lateral shoots was 35.6%, while that in the upper part was 30.8%.

Then, thioacidolysis and GC–MS analysis were performed on samples A-1, A-3, B, and lateral shoots. The yields of thioacidolysis monomeric products obtained are shown in Fig. 10 and Additional file 1: Table S1. The chi-chi samples each yielded ca. 400–550 μmol/g of G-unit, and the lateral shoot samples yielded about 400 μmol/g of G-unit. In terms of H-unit yield, no H-unit was detected in sample B, in which the growth axes of the tracheids and ray cells were similar to that of the normal trunk. In contrast, approximately 30 μmol/g

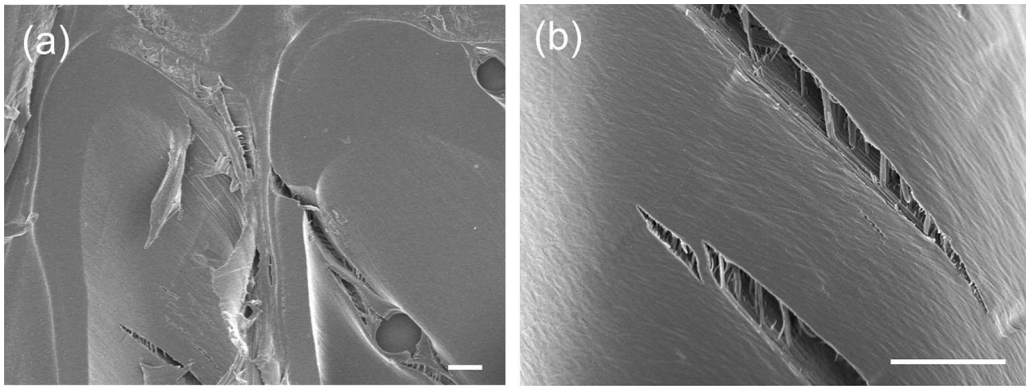

Fig. 7 FE-SEM micrograph of the cell wall of sample A-2 in Fig. 3b. The image shows the lack of an S_3 layer, and S_2 layer microfibrils were oriented in Z-helix with 45°. Scale bar, 3 μm

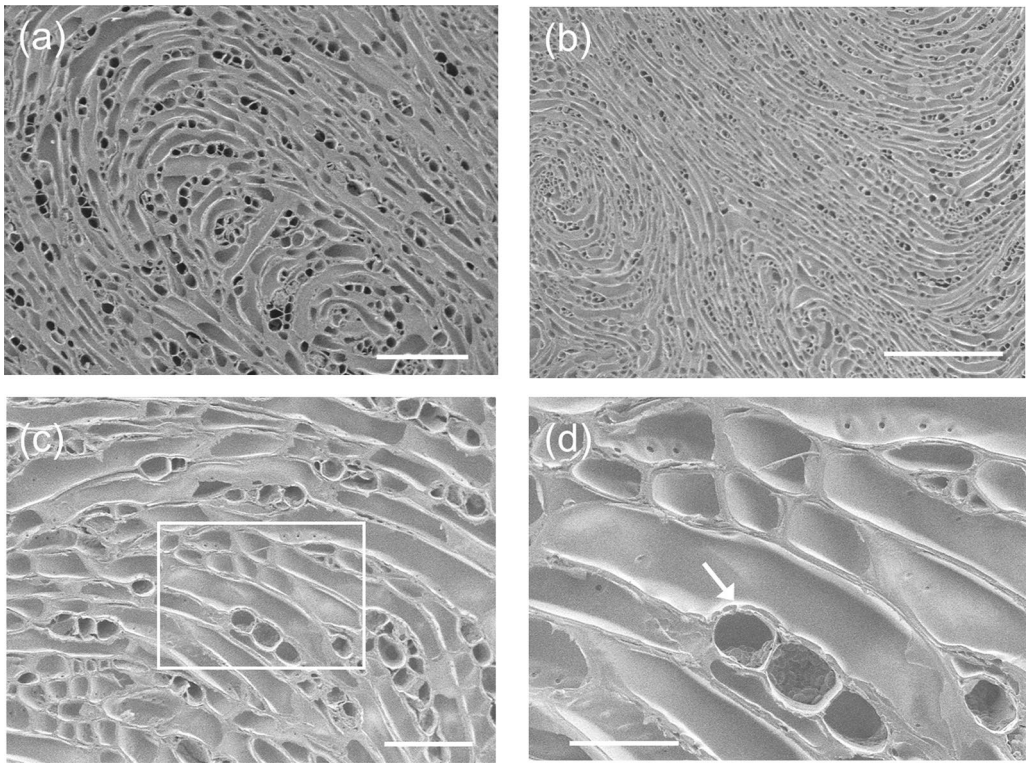

Fig. 8 SEM micrographs of the swirls, curving tracheids, and rays in Sample C. **a** SEM micrograph of the swirl in a horizontal plane at 30 mm from the tip of the chi-chi (sample C). Scale bar; 200 µm. **b** A wide-angle view taken in a horizontal plane at 30 mm from the tip of the chi-chi (sample C) shows several swirls contiguous to each other. Scale bar, 500 µm. **c** SEM micrograph of the swirl of tracheids in a horizontal plane and cross-sectioned ray at 30 mm from the tip of the chi-chi of sample C. Scale bar, 100 µm. **d** An enlarged image of the area outlined by the white rectangular area in (**c**). Tracheids with bordered pits linked uniseriate rays with cytoplasmic debris (white arrow). Scale bar, 50 µm

was detected in samples A-1 and A-3, where the curving tracheids were observed. In the lateral shoot samples, H-unit yield was higher in the lower part, i.e., usual ginkgo compression wood, with 51 µmol/g. The H-unit composition ratio [= H-unit/(G-unit + H-unit)] was 12%. This value is close to the H-unit composition ratio of 14% reported for spruce compression wood [16]. The ratio of H-unit in the chi-chi sample was 5.9% and lower than that in the lateral shoot.

Thioacidolysis results from small blocks are summarized in Fig. 10 and Additional file 1: Table S1. G-unit was detected in all blocks, ranging from 300 to 480 µmol/g. No H-unit was detected in the upper small blocks (Da, Db, Dc, Dd, De, Df, Dg, and Di). H-units were detected in 12–19 µmol/g in small blocks (Dh, Dj, Dk, and Dl) sampled from the lower part. In the blocks where H-units were detected, the composition ratio was about 4%.

Finally, the thioacidolysis dimeric product analysis result is listed in Additional file 1: Table S2. There were no significant differences in the composition of dimer linkage types (5–5′, 4-*O*-5′, β-1′, β-5′, and β–β′) within the chi-chi and lateral shoot samples.

Discussion

Barlow and Kurczyńska [3] proposed a growth mechanism in which chi-chi elongates downward by the cambium. They described "tracheids show variable orientations" and suggested "a swirl of tracheids may indicate initiation of a woody nodule." Here, a "nodule" was reported as a tissue having disturbed and horizontal arrangements of tracheids, and it was estimated as a result of the specific growing behavior of the chi-chi tissue. They called the small object on the chi-chi surface as woody spines and did not mention the relationships with growing mechanisms.

These descriptions of the chi-chi tissues agree with our results in this study to some extent. In this study, the internal microstructure of the chi-chi was observed by microscopic observations and X-ray µCT. Here, we take a step forward about the chi-chi elongation mechanisms. There are three significant points. First, the surface small object was not woody (lignified) spines but parenchymatous ones; we called the object as latent buds. Second, the center of the tracheid swirling might be the parenchymatous latent bud tissue. Third, the swirls are continuous over a millimeters scale, and several swirls construct a

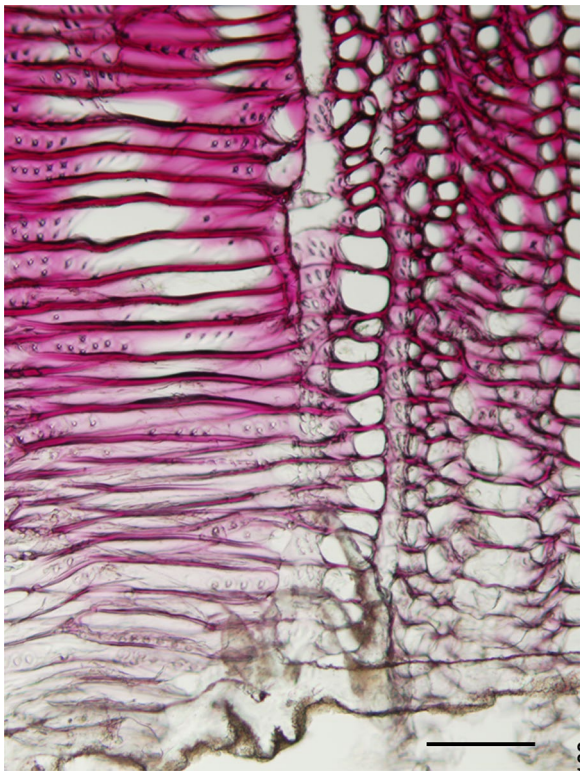

Fig. 9 Photomicrograph of radial section of the tip of sample C. The section was 20 µm-thick and stained with phloroglucinol hydrochloric acid. Left-side tracheids cut axially show bordered pits. In contrast, tracheids on the right side are cut in a cross-section. The bark side is down below. Scale bar, 100 µm

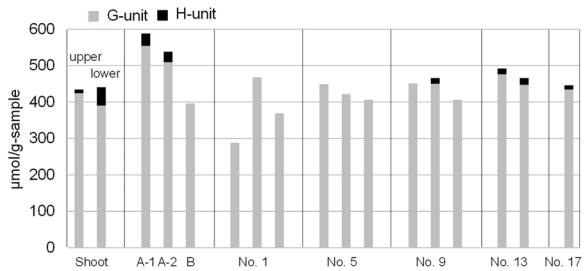

Fig. 10 Yields of thioacidolysis monomeric products. Values are obtained for the chi-chi (A-1, A-3, B, and separated D samples) and the lateral shoot (upper and lower parts) samples. Chi-chi sample codes are illustrated in Figs. 2, 3, 4. The resultant values are summarized in Additional file 1: Table S1

woody bulge. From these observations, we estimated that the cambium around the woody bulges with latent buds drives the downward growth of the chi-chi.

Generally, compared to normal wood, compression wood tracheids are rounded in the transverse section, and intercellular spaces between the corners of adjacent cells occur in it. These tracheids are thick-walled and have higher lignin content with significant *p*-hydroxyphenyl subunits. The S_3 layer is absent, and the S_2 layer microfibril orientation is close to 45°. For the curving tracheids in the chi-chi, there was no S_3 layer, and the S_2 layer microfibril orientation was 45°. This is not the helical cavity but should be the spiral drying check of S_2 layer due to drying of the sample, as reported previously [6, 7], or the possible physical stresses within the sectioning processes. To the best of our knowledge, this is the first reported case of the absence of S_3 in the cell wall structure of a curved tracheid. The absence of the S_3 layer is an essential early anatomical change in the transition of normal wood to compression wood [17]. Although cell wall thickening and shape rounding of the curving tracheids were not observed, some compression-wood-like features are thought to be expressed.

Another parameter that differentiates the chi-chi tissue from normal ginkgo wood is the lignin chemical structure. The lignin composition and lignin content of the chi-chi was heterogeneous and differed between the upper and lower parts, with the lower tip tending to have more H-unit and lignin content, indicating that it has compression-wood-like features. This result is consistent with the SEM image in Fig. 6, which shows that the tracheids of sample B in the upper part of chi-chi are aligned parallel to the gravity direction and similar to normal wood.

As reported by Sinnott, it has been shown that when a conifer branch is artificially looped in the horizontal plane, compression woods are formed inside the loop [18]. In the horizontal plane of the chi-chi tip, the swirl formation by curving tracheids may have had some stress effect on cell wall formation and contributed to the triggering of the compression wood formation.

For the tracheary element swirls in the secondary xylem, Rothwell et al. reported the presence of the circular tissue in the tangential section of the secondary xylem of 375 million-year-old fossil wood of *Archaeopteris*, as well as in the present woody *Spermatophyta* [19, 20]. They attributed this to the formation of auxin whirlpools due to the obstruction of axial polar transport of auxin by buds and branches. The swirls of chi-chi tracheids in the horizontal plane may be caused by latent buds, with a mechanism similar to the auxin whirlpools in the vertical plane proposed by Rothwell et al. [20].

The enlarged SEM image of the area suggested by white rectangles in Fig. 8c shows that curving tracheids have bordered pits (Fig. 8d). Here, these ray cells intersected the curving tracheids; therefore, the axis of the ray cells was parallel to the gravity direction. Ray cells exist in the horizontal plane in the normal trunk but in the vertical plane at the chi-chi tip. This spatial arrangement may

suggest some possible mechanisms in which an orthogonal relationship between tracheids and rays is preferentially maintained in tissue development, regardless of the direction of gravity in the space where the tracheids are located.

Conclusion

The elongation of the chi-chi can be classified into two stages. Near the tip growing part of the chi-chi, multiple aggregates of tracheids curving in the horizontal plane and intersecting ray cells, i.e. swirls, have a parenchymatous tissue of latent bud in the center and form wood. This results in the growth of woody bulges, and the chi-chi grows downward.

Tracheids in the swirl have no S_3 layer in their cell wall structure and have H-units in the lignin chemical structure. However, the cell walls of the curved tracheids were not thickened, not rounded, and had no intercellular spaces; therefore, they have only a part of gymnosperm compression-wood-like features. With time, the growing axes of tracheids and ray cells in chi-chi become similar to those in normal wood of the stem, and the lignin is composed only of G-units.

Abbreviations

GC–MS	Gas chromatography-mass spectrometry
SEM	Scanning electron microscopy
FE-SEM	Field-emission SEM
X-ray µCT	X-ray micro-computed tomography
MFA	Microfibril angle
MWL	Milled wood lignin
H	*p*-Coumaryl alcohol
G	Coniferyl alcohol
S	Sinapyl alcohol

Supplementary Information

The online version contains supplementary material available at https://doi.org/10.1186/s10086-023-02102-4.

Additional file1: Fig. S1. The elder *G. biloba* tree in Kitakanegasawa (a natural monument). **Fig. S2.** Latent buds and hollows of the chi-chi. **Fig. S3.** Photomicrographs of the latent bud in the tip of sample E. **Fig. S4.** Sample A before cut underpart. **Fig. S5.** FE-SEM micrographs of the cell wall of the chi-chi sample. **Fig. S6.** SEM micrographs of the swirls. **Table S1.** Lignin content and yields of thioacidolysis monomeric products. **Table S2.** Yields of thioacidolysis dimeric products.

Additional file 2: Fig. S7. Cross-sectional consecutive screen movie of the sample C by X-ray µCT.

Acknowledgements

The authors thank K. Shinoda, Chairman of Neighborhood Association of Kasamatsu-cho Kamishin-machi, Gifu Prefecture, Japan, for the sampling permission of the chi-chi; S. Sakamoto, Superintendent of Education, Fukaura-cho, Aomori Prefecture, Japan, for the permission for the on-site survey of the elder *G. biloba* tree in Kitakanegasawa; S. Kimura and R. Fujita, Nikon Instech co. Ltd, Japan, for conducting X-ray µCT analysis. The authors sincerely thank N. Terashima, the professor emeritus, Nagoya University, Japan, for his experimental and research advice.

Author contributions

SH, DA, YM, and KF conceived the research. SH, YM, and KF conducted sampling. SH and SY conducted chemical analyses. SH and MY performed microscopic observations. SH and DA wrote the manuscript. All authors read and contributed to the manuscript.

Funding

This work was supported by JSPS KAKENHI Grant numbers 25252032, 18H03959, and 23H02275.

Availability of data and materials

The data sets analyzed during the current study are available from the corresponding author on reasonable request.

Declarations

Competing interests

The authors declare that they have no competing interests.

Received: 4 May 2023 Accepted: 10 August 2023
Published online: 30 August 2023

References

1. Fujii K (1895) On the nature and origin of so-called "Chichi" (nipple) of *Ginkgo biloba*, L. Bot Mag 9:440–444. https://doi.org/10.15281/jplantres1887.9.440
2. Li Z, Lin J (1991) Wood anatomy of the stalactite-like branches of Ginkgo. IAWA J 12:251–255. https://doi.org/10.1163/22941932-90001252
3. Barlow PW, Kurczyńska EU (2007) The anatomy of the chi-chi of *Ginkgo biloba* suggests a mode of elongation growth that is an alternative to growth driven by an apical meristem. J Plant Res 120:269–280. https://doi.org/10.1007/s10265-006-0050-3
4. Del Tredici P (1992) Natural Regeneration of *Ginkgo biloba* from downward growing cotyledonary buds (basal chichi). Am J Bot 79:522–530. https://doi.org/10.2307/2444863
5. Timell TE (1960) Studies on *Ginkgo biloba*, L. 1. General characteristics and chemical composition. Svensk Papperstidning 63:652–657
6. Timell TE (1978) Ultrastructure of compression wood in *Ginkgo biloba*. Wood Sci Technol 12:89–103. https://doi.org/10.1007/BF00350815
7. Timell TE (1986) Compression wood in gymnosperms. Springer, Berlin, Heidelberg
8. Groover A (2016) Gravitropisms and reaction woods of forest trees—evolution, functions and mechanisms. New Phytol 211:790–802. https://doi.org/10.1111/nph.13968
9. Dimmel DR (2010) Overview. In: Heitner C, Dimmel DR, Schmidt JA (eds) Lignin and Lignans. CRC Press, Boca Raton, pp 1–10
10. Uzal EN, Gómez Ros LV, Pomar F, Bernal MA, Paradela A, Albar JP, Barceló AR (2009) The presence of sinapyl lignin in *Ginkgo biloba* cell cultures changes our views of the evolution of lignin biosynthesis. Physiol Plant 135:196–213. https://doi.org/10.1111/j.1399-3054.2008.01185.x
11. Iiyama K, Wallis AFA (1988) An improved acetyl bromide procedure for determining lignin in woods and wood pulps. Wood Sci Technol 22:271–280. https://doi.org/10.1007/BF00386022
12. Fukushima RS, Hatfield RD (2001) Extraction and isolation of lignin for utilization as a standard to determine lignin concentration using the acetyl bromide spectrophotometric method. J Agr Food Chem 49:3133–3139. https://doi.org/10.1021/jf010449r
13. Lapierre C, Monties B, Rolando C (1986) Preparative thioacidolysis of spruce lignin: isolation and identification of main monomeric products. Holzforschung 40:47–50. https://doi.org/10.1515/hfsg.1986.40.1.47
14. Lapierre C, Pollet B, Monties B (1991) Thioacidolysis of spruce lignin: GC-MS analysis of the main dimers recovered after Raney nickel desulphuration. Holzforschung 45:61–68. https://doi.org/10.1515/hfsg.1991.45.1.61

15. Lapierre C, Pollet B, Rolando C (1995) New insights into the molecular architecture of hardwood lignins by chemical degradative methods. Res Chem Intermed 21:397–412. https://doi.org/10.1007/BF03052266
16. Lapierre C (2010) Determining lignin structure by chemical degradations. In: Heitner C, Dimmel DR, Schmidt JA (eds) Lignin and lignans. CRC Press, Boca Raton, pp 11–48
17. Abe H, Funada R (2005) Review—the orientation of cellulose microfibrils in the cell walls of tracheids in conifers: a model based on observations by field emission-scanning electron microscopy. IAWA J 26:161–174. https://doi.org/10.1163/22941932-90000108
18. Sinnott EW (1952) Reaction wood and the regulation of tree form. Am J Bot 39:69–78. https://doi.org/10.2307/2438096
19. Rothwell GW, Lev-Yadun S (2005) Evidence of polar auxin flow in 375 million-year-old fossil wood. Am J Bot 92:903–906. https://doi.org/10.3732/ajb.92.6.903
20. Rothwell GW, Wyatt SE, Tomescu AMF (2014) Plant evolution at the interface of paleontology and developmental biology: an organism-centered paradigm. Am J Bot 101:899–913. https://doi.org/10.3732/ajb.1300451

Publisher's Note